Med Biol Eng Comput
DOI 10.1007/s11517-009-0543-z

ORIGINAL ARTICLE

Theoretical evaluation of a simple cooling pad for inducing hypothermia in the spinal cord following traumatic injury

Katisha D. Smith · Liang Zhu

Received: 12 May 2009 / Accepted: 23 October 2009

Abstract The Pennes bioheat equation and finite element method (FEM) are used to solve for the temperature distributions in the spinal cord and cerebrospinal fluid (CSF) during 30 min of cooling for spinal cord injury (SCI) patients. The average CSF and spinal cord temperatures are reduced by 3.48 and 2.72°C, respectively. The 100-mm wide pad provides the desired cooling and uses the least amount of material. The presence of zero-average CSF oscillation under normal conditions decreases the cooling extent in the spinal cord due to the introduction of warm CSF surrounding the spinal cord. The temperature decrease in the spinal cord is more than doubled when the temperature at the back of the torso is lowered from 20 to 0°C. Spinal cord ischemia, often observed after traumatic spinal cord injury, promotes cooling penetration. The proposed technique can reduce the spinal cord temperature by 2°C within 30 min and may be a feasible treatment for traumatic SCI.

Keywords Spinal cord injury · Cerebrospinal fluid · Hypothermia · Temperature · Heat transfer

1 Introduction

Each year in the United States, one in every 1,000 individuals suffers from spinal cord injury (SCI) [24]. These injuries can be caused by both traumatic and non-traumatic events. However, approximately 90% of all SCIs stem from trauma that causes dysfunction of the cord and lead to loss of sensory and motor function. Such events include motor vehicle accidents (47%), acts of violence (7%), falls (12%), and sports (24%) [24]. According to the National Spinal Cord Injury Database, nearly 50% of all those suffering from SCI result in permanent damage. In addition to the initial physical damage, secondary injury can cause additional neurological damage. Usually, secondary neuro-injury occurs within the first 12–24 h following injury, but it can also last up to 5–10 days for more severe injuries [24]. These injuries initiate a cellular inflammatory response at the injury site and increase the release of damaging free radicals. These free radicals contribute to tissue ischemia, cerebral edema, and disruption of the spinal cord–blood barrier. Therefore, it is essential to develop an effective method to treat traumatic SCI and prevent subsequent secondary neuro-injury.

In addition to conventional treatments for traumatic SCI, hypothermia has been widely studied as a beneficial approach because of the neuro-protection it provides against secondary injury. Both clinical studies and animal experiments have shown that the benefits of hypothermia include reducing oxygen consumption, decreasing free radical generation, delaying the release of damaged neurotransmitters, reducing inflammation, lowering metabolic demand, and preventing cytotoxic edema [6, 27, 48, 50, 51, 55]. Even a temperature reduction of 1–2°C has been demonstrated to be beneficial against secondary neuro-injury at the cellular level in any organ or tissue [27, 55]. However, the major challenge is to develop a cooling protocol that can be initiated as early as possible, cool tissue quickly, and provide a uniform temperature reduction. Both systemic and selective hypothermia have been shown to prevent permanent neurological tissue damage following traumatic injury.

Popular systemic cooling techniques include wrapping the body in a cooling blanket, immersing the body in cold

K. D. Smith · L. Zhu (✉)
Department of Mechanical Engineering, University of Maryland, Baltimore County, 1000 Hilltop Circle, Baltimore, MD 21250, USA
e-mail: zliang@umbc.edu

Published online: 15 October 2009

water, or packing the body with ice. It has been shown that systemic cooling hinders the re-entrance of damaged neurotransmitters into the spinal cord and increases spinal cord blood flow, as well as improves spinal cord cell survival rate [9, 19, 52, 55]. However, inducing whole body cooling in humans can lead to adverse consequences. Severe decreases in the core body temperature, which are often associated with inducing systemic hypothermia, can lead to dangerous complications, such as reducing cardiac output, increasing blood viscosity, shivering, increasing cardiac arrhythmias, and even death [7, 29]. The procedure of inducing whole body cooling in humans presents a reverse benefit–risk ratio and decreases its ability to be safely implemented in a clinical setting [39].

In order to avoid the complications associated with systemic hypothermia and to only cool the injured spinal cord, it may be more beneficial to apply selective hypothermia. This method allows the core body temperature to remain at 37°C while the spinal cord temperature is reduced. Localized cooling can still protect the spinal cord from permanent neurological damage while reducing the unnecessary cooling to the rest of the body and avoiding adverse side effects. Studies have shown that selective hypothermia can provide the same benefits as systemic hypothermia, such as reducing spinal cord swelling and improving spinal cord blood flow [3, 4, 8, 14, 47, 48]. Albin et al. first documented a successful application of localized spinal cord cooling for experimental SCI in dogs by perfusing the injured spinal cord with isotonic saline (5°C) for 2.5 h [2]. Since then, there have been a number of promising experimental animal studies using similar cooling methods [1, 3, 4, 7, 9]. Recently, two other successful cooling techniques have been developed, which include using an epidural cooling catheter [34, 37, 42] and placing a cooling saddle directly onto the spinal cord [12, 14, 17, 18, 51]. Despite the promising results in both animal and clinical experimentation, the major disadvantages of these localized cooling protocols are the invasive techniques implemented. In order to insert the cooling devices such as the epidural catheter and the cooling saddle, a laminectomy is performed, where the back of one or more vertebrae is removed to give access to the spinal cord. This surgery may cause additional physical trauma and may delay cooling initiation [35]. Although there is a select group of SCI patients who must undergo surgical decompression of the spine, and integrating hypothermia treatment may be beneficial for them, laminectomies for the sole purpose of inducing localized spinal cord cooling are rarely performed [25]. Therefore, previously presented procedures of locally cooling the spinal cord cannot be readily implemented. Currently, there are no studies that explore the option of inducing local spinal cord cooling without surgical intervention.

The objective of this article is to determine the feasibility of reducing the spinal cord temperature by 2°C within a 30-min duration using a cooling pad. The cooling pad is placed on the back of the torso along the spine. Theoretical simulations are performed to predict the temperature distributions in the torso region. Parametric studies are conducted to test the sensitivity of the cooling extent in the spinal cord to several design parameters and physiological conditions.

1.1 Theoretical model of human torso

The spinal cord is a long, thin, tubular bundle of nerves that extends the central nervous system (CNS) from the brain and is enclosed and protected by the spinal column. Its main function is to transmit neural inputs between the peripheral nervous system and the brain. The human spinal cord weighs approximately 35 g, and its average length is around 50 cm [15, 32]. Similar to the brain, it is composed of both gray and white matter. The grey matter is located in the center and surrounded by the white matter. The cerebrospinal fluid (CSF) moves within the cavity surrounding the spinal cord. CSF is a dynamic fluid that is produced by the ependymal cells of the choroids plexus inside the ventricles of the brain and flows through the cavities surrounding the brain and the spinal cord. The purpose of CSF is to act as a buffer and the plumbing system for the CNS. The major function of CSF is to provide mechanical and immunological protection to the brain and the spinal cord.

Several research studies have shown that CSF flow correlates with the cardiac cycle due to changes in the intracranial pressure (ICP) within the brain [5, 13, 38]. As shown in Fig. 1, CSF takes two routes, one within the brain cavity and the other in the spinal cavity. During arterial systole, there is an increase in blood flow to the brain, which results in an increased ICP and prompts the release of CSF from the ventricles. From there, CSF flows into the spinal cavity toward the sacral sac and through the cavity surrounding the brain (*left*). Arterial diastole during the cardiac cycle decreases ICP and allows CSF to flow in the opposite direction from the sacral sac located at the base of the spinal cavity toward the brain where a smaller amount of the CSF enters the brain cavity. As CSF flows within the brain cavity, some of the CSF is absorbed into the venous bloodstream through the arachnoid granulations located at the top of the brain cavity (*right*). After a certain time, the small absorption of CSF will decrease the total amount of CSF in the CNS. In order to maintain the total volume of CSF within the human body, 125–150 ml, the choroids plexus produce 0.35 ml of CSF each minute to compensate for fluid absorption [13, 32, 43, 44]. CSF absorption and production are a very slow process, and it takes more than 6 h to completely replace all the CSF in the body.

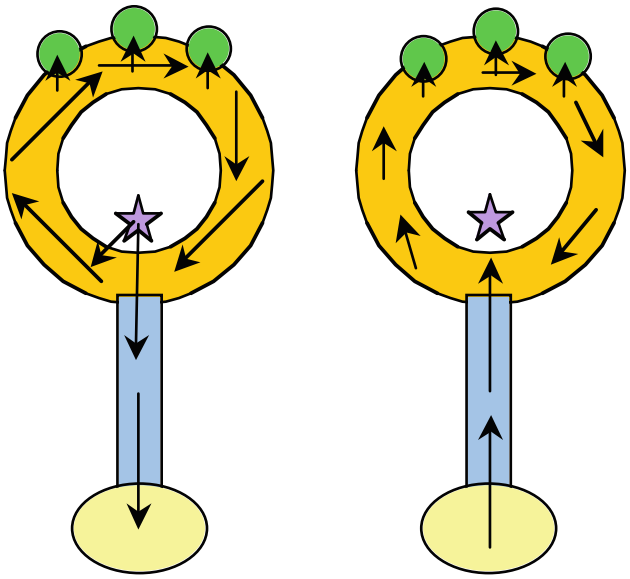

Fig. 1 Schematic diagram of CSF flow within the CNS during arterial systole (*left*) and arterial diastole (*right*). Green circle—Arachnoid granulations, Orange circle—Brain cavity, White circle—Brain, Purple star—Ventricles, Blue rectangle—Spinal cavity, Yellow oval—Sacral sac

In addition to the ICP, compliance in the brain and the spinal cavities and changes in body position also influence CSF motion. Total compliance of both cavities is independent of body position, but the compliance relationship between the two cavities depends on body position [33]. When the body is in a horizontal body position, the total amount of CSF in the brain and spinal cavities is 37 and 63%, respectively [33]. In a standing position, the percentages are nearly reversed: 66% for the brain cavity and 34% for the spinal cavity [33].

CSF motion within the spinal cavity has periodic oscillation, but the net flow rate is close to zero [32, 40], and CSF production is a slow process. Movement within the cavity is mostly up and down, and changes in the flow rate are mostly due to postural changes, the cardiac cycle, respiration, and coughing [40]. There is a decrease in its velocity descending down the spine, but there are also indications of fluid acceleration in the spinal cavity near the skull and at the base of the spine [32, 40]. This can be attributed to the changes in the cardiac cycle, as well as the non-uniform cross-sectional area of the spinal cavity.

A three-dimensional model of the human torso is developed in this study for simulating spinal cord hypothermia and is shown in Fig. 2. The torso is modeled as a rectangular column. The spinal column, the spinal cavity housing the CSF, and the spinal cord are embedded within the torso as concentric tubes. The spinal column, composed of bone and cartilage, is simplified as a homogenous cylinder with a constant cross-sectional area. The cylindrical-shaped spinal cord has also been simplified by not distinguishing between the gray and the white matters. The rest of the torso is modeled as muscle tissue.

All the thermal properties are assumed to be homogeneous and isotropic, and the Pennes bioheat equation for the tissue structures is as follows:

$$(\rho c)_{sp,bo,m}\frac{\partial T_{sp,bo,m}}{\partial t} = k_{sp,bo,m}\nabla^2 T_{sp,bo,m} + (\rho c)_{bl}\omega_{sp,bo,m}\left(T_a - T_{sp,bo,m}\right) + q_{msp.bo,m} \quad (1)$$

The governing equation for the CSF consists of heat conduction terms for an isotropic material, and a convection term due to the oscillating CSF motion and is given by:

$$(\rho c)_{\mathrm{csf}}\frac{\partial T_{\mathrm{csf}}}{\partial t} = k_{\mathrm{csf}}\nabla^2 T_{\mathrm{csf}} - (\rho c)_{\mathrm{csf}}u_{\mathrm{csf}}\nabla T_{\mathrm{csf}} \quad (2)$$

The subscripts *sp*, *bo*, *m*, *bl*, and *csf* represent spinal cord, bone, muscle, blood, and cerebrospinal fluid, respectively, k is the thermal conductivity, ρ is the density, c is the specific heat capacity, ω is the local blood perfusion rate, and q_{m} is the local volumetric heat generation rate. In Eq. 2, u_{csf} is the velocity of the CSF in the axial direction and is simplified by varying only as a function of time. In this study, the arterial blood temperature, T_{a}, in Eq. 1 is assumed to equal 37°C, the core body temperature.

There are five prescribed boundary conditions for the system, as shown in Fig. 3. The thermal effect of the cooling pad is modeled as a constant temperature (T_{cool}) at the pad–torso interface. The bottom surface of the torso is assumed to equal the core body temperature, 37°C, under normal conditions. Separate boundary conditions are prescribed for the top torso surface. The top surface of the CSF

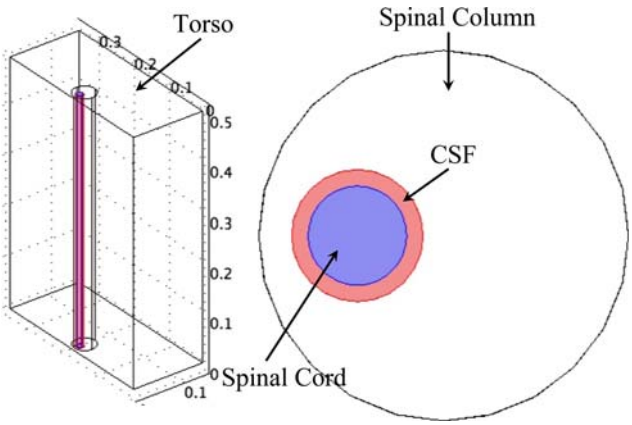

Fig. 2 Schematic diagram of the torso region. The torso is modeled as a rectangular prism. The spinal column (*white*), spinal cord (*blue*), and CSF (*red*) are embedded in the prism and are modeled as concentric circular cylinders. The cross section of the embedded anatomy has been enlarged to show the detail

has a special prescribed boundary condition known as a convective flux because the convective heat transfer dominates the conduction heat transfer of the fluid in the axial direction. The peak Peclet number ($Pe^* = 4100$) for the CSF is calculated using the expression, $VL\alpha^{-1}$ [26, 57], where V is the peak CSF velocity (0.0764 m/s), L is the characteristic length (0.008 m), and α is the thermal diffusivity (1.4906e−7 m^2/s). Since the Peclet number is much larger than unity in the current application, the axial conduction of the fluid can be neglected. The top surface at the neck-torso interface is assumed adiabatic. This is based on previous simulation results [49] showing that the conduction through that interface is almost negligible. The area representing the human shoulders is subjected to radiation and natural convection from the surrounding environment. The remaining side surfaces of the torso are also subjected to radiation and natural convection from the surrounding environment. The ambient temperature of the environment is prescribed as $T_\infty = 25°C$, and the overall heat transfer coefficient is calculated as $h = 9.99$ W/m^{2}K ($h_{rad} = 6.19$ W/m^{2}K and $h_{conv} = 3.80$ W/m^{2}K) [26]. The initial condition of the model domain is the sustained temperature field prior to cooling.

Temperature distributions in the torso region are solved using finite element method (FEM). All the finite element calculations and mesh generation are performed using FEMLAB 3.1 (COMSOL, Stockholm, Sweden) on an Apple PowerBook G4 (Mac OS 10.4, 2 GB RAM, 1.67 GHz processor), an Apple Intel iMac (Windows XP SP2, 2.8 GHz processor, 1.5 GB RAM), and a Dell Pentium IV (Windows XP SP2, 2.79 GHz processor, 2 GB RAM). The numerical model of Eqs. 1 and 2 are obtained by applying the Generalized Minimal Residual (GMRES) method with an Incomplete LU pre-conditioner (0.0001 absolute tolerance and 0.001 relative tolerance). Only half of the torso geometry is included in the numerical model to accord with geometric symmetry and to conserve computational memory. The final mesh contains 180,611 tetrahedral Lagrange linear elements and is shown in Fig. 4. The independency of the volumetric mesh is tested by increasing the number of elements of the initial mesh (87,566 elements) by approximately 100% (180,611 elements). The results are compared to the initial mesh, and the finer mesh results in a less than 1% error in the global temperature distributions for the spinal cord and CSF, and also reaches the limit of the available computational memory capacity. The sensitivity of the time interval used during transient analysis is also tested by decreasing the time step by 50%, from 0.25 to 0.125 s. This test helps determine how small the time interval must be in order to show the subtle temperature changes occurring in the tissue during transient heat transfer. The temperature profiles using both intervals showed a difference of less than 1% in the temperature profile, and, hence, a time interval of 0.25 s is used to predict the transient heat transfer process in the system.

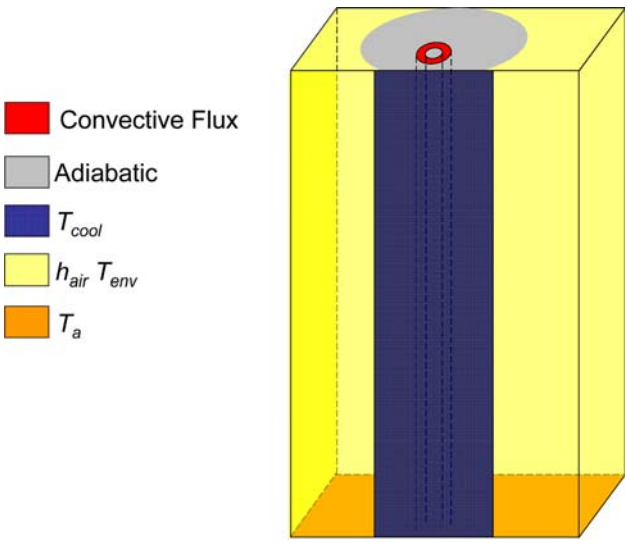

Fig. 3 Schematic diagram of the torso region with prescribed boundary conditions. The five prescribed boundary conditions are the cooling temperature, T_{cool}, at the pad-torso interface (*blue*), thermal insulation of tissue at the neck–torso interface (*gray*), convective flux of CSF at the neck–torso interface (*red*), temperature of bottom torso surface, T_a (*orange*), and radiation and natural convection from the surrounding environment (*yellow*)

2 Results

The physical and physiological parameters under normal conditions used in the torso model can be found in previous

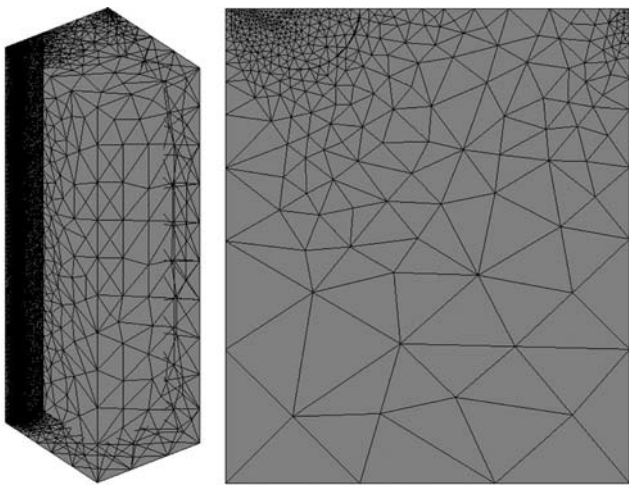

Fig. 4 Schematic diagram of volumetric mesh. The final mesh consists of 180,611 tetrahedral elements, which represents a 100% increase in the number of elements from the initial mesh of 87,566 elements. The mesh cross section is shown on the right

studies [11, 14, 32, 49, 54, 58] and are listed in Table 1. Note the high metabolic heat generation rate and the high local blood perfusion rate in the spinal cord. The equivalent blood perfusion rate in the spinal cord is 50 ml/min/100 g tissue, which is similar to that in the normal brain tissue. Although the torso consists of both muscle and internal organs, in this study, we assume that it has the blood perfusion rate of muscle tissue. This is justified since cooling only affects a limited region close to the back of the torso. Table 2 shows the geometrical parameters of the torso region. The disks of the spinal column are approximated as a circular column to overcome the 3D computational resource limitations. Although the realistic cross section of the spinal column is not circular, this assumption can be justified to ensure that the overall heat transfer resistance by the spinal disk is modeled correctly.

The frequency of the CSF flow corresponds with the human heartbeat, and it is necessary to model the pulsating flow within the spinal cavity. Modeling the hydrodynamic CSF motion within the spinal cavity shows that the peak flow rate for the CSF is 360 ml/min and illustrates that the net flow of the CSF is zero [32], which can be represented using a sine function with a frequency of 1 Hz. Therefore, in this study, the CSF velocity, u_{csf}, under normal conditions is calculated and is given by

$$u_{csf} = 0.0764 \sin(2\pi t) m/s \quad (3)$$

The baseline for the torso region model consists of the cooling pad ($T_{cool} = 20°C$, 500 mm long and 100 mm wide), and the cooling process is simulated for 30 min. Figure 5 shows the temperature contours of the midline axial and sagittal cross sections after 1800 s of cooling. After a 30-min hypothermia treatment, cooling penetration is evident. As shown by the light red color in the spinal cord, the temperature in the spinal cord region is reduced to approximately 34°C. The temperature in the CSF is approximately 33°C after 30 min of cooling. There is significant cooling in both the spinal cord and the CSF. The temperature at the back surface is 20°C due to the cooling pad, which then increases through the spinal column and neck region, and one observes an almost uniform temperature reduction in the CSF. However, in the spinal cord region, the temperature is higher than the temperature of the surrounding CSF. This may be largely due to the high metabolic heat generation and blood perfusion rates in the spinal cord. Both act as a heat source to the local temperature field. The presence of warm arterial blood in the highly perfused spinal cord tissue region is counterproductive to cooling.

As the spinal cord and the CSF are the targeted regions for the cooling protocol, their average temperatures during the transient process are illustrated in Figure 6, which gives a representation of the cooling occurring during the 1800-s time frame. Although the CSF velocity oscillates at a frequency of 1 Hz, this oscillation does not result in visible fluctuations at that frequency in the tissue and the fluid temperatures during cooling. This may be due to the fact that human tissue has a very high thermal capacity, which requires a very low frequency to cause significant oscillations in temperature. After 30 min, temperatures within both the spinal cord and the CSF have not established a steady state, suggesting that a longer cooling duration may further lower the tissue temperature. After the hypothermia treatment, the average temperature reduction in the CSF and the spinal cord from their initial values are 3.48 and 2.72°C, respectively. The temperature reduction in the CSF is nearly 1°C more than that of the spinal cord. The current

Table 2 Geometrical parameters of torso model

Parameter	Length (mm)	Width (mm)	Height (mm)	Radius (mm)
Torso	350	150	500	–
Spinal column	–	–	500	22.5
Spinal canal	–	–	500	8
Spinal cord	–	–	500	6

Table 1 Physical and physiological parameters under normal conditions in baseline model

Parameter	Specific heat capacity, c (W/kgK)	Density, ρ (kg/m^3)	Thermal conductivity, k (W/mK)	Local blood perfusion rate, ω (1/s)	Local volumetric heat generation, q_m (W/m^3)	Velocity, u (m/s)
Blood	3800[a]	1050[a]	–	–	–	–
Muscle	3700[d]	1050[d]	0.5[d]	1.67e−4[d]	180.2[d]	–
Bone	2300[a]	1500[a]	1.12[a]	3e−4[a]	368.3[a]	–
CSF	4178.3[b]	1000.3[b]	0.623[b]	–	–	0.0764sin(2πt)[c] $Pe^* = 4100$
Spinal cord	3700[a]	1050[a]	0.5[a]	0.0083[a]	10437.5[a]	–

[a] [11], [b] [14], [c] [32], [d] [49]

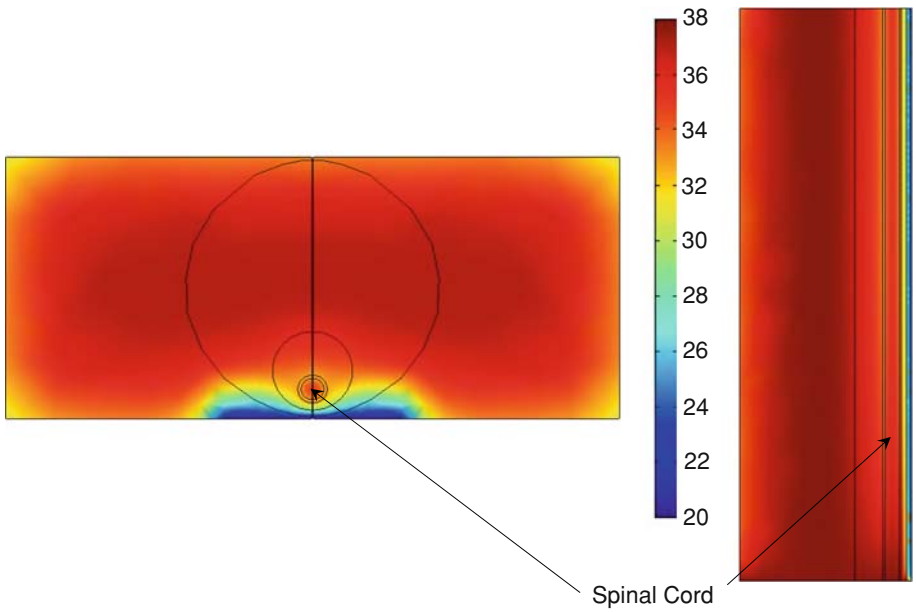

Fig. 5 Temperature contours for the midline axial (*left*) and sagittal (*right*) cross-section of the torso region after 30 min of cooling

procedure satisfies the design requirement of decreasing the spinal cord temperature by 2°C within 30 min.

Parametric studies are used to test the sensitivity of various design and physiological parameters on the simulated temperature distributions. The parameters tested for this study include the cooling pad width, the cooling temperature, the CSF velocity, and the local spinal cord blood perfusion rate, which are considered the most influential factors. Table 3 highlights the results of the parametric study, and the baseline parameters are depicted in bold. The results help optimize the cooling pad design and understand the cooling potential.

Decreasing the pad width does not change the results significantly until it becomes very narrow ($\sim$50 mm). The 100-mm wide pad satisfies the design requirements while using the least amount of material, and the remaining parametric studies are performed using this pad width.

Changes in the CSF velocity can be attributed to various factors including disease, ICP, and body position. This parametric study determines whether the oscillatory CSF motion enhances convective heat transfer within the system. The results support that a slow CSF motion enhances the cooling extent to the spinal cord. Under normal conditions, $u_{csf} = 0.0764\sin(2\pi t)$, the temperature reduction in the spinal cord is 2.72°C. When the CSF peak velocity decreases by 50%, the achievable temperature reduction in the spinal cord, ΔT_{sp}, is increased to 2.91°C, and a 75% decrease in the CSF velocity achieves a spinal cord temperature reduction of 3.05°C.

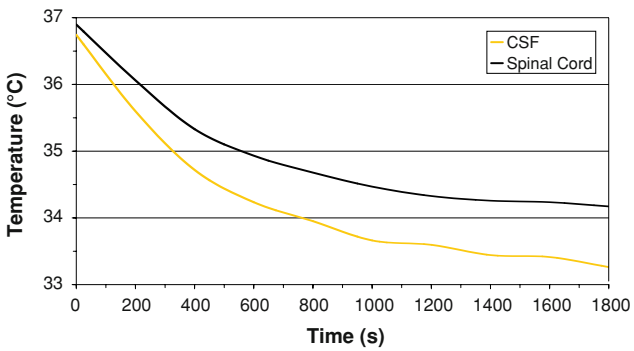

Fig. 6 Average transient temperatures of spinal cord and cerebrospinal fluid during the 30-min hypothermia treatment

In order to cool the spinal cord, a significant temperature gradient between the spinal cord tissue temperature and the surface tissue temperature is required. Therefore, the cooling pad temperature must be low enough to induce hypothermia within the spinal cord, as well as within the CSF. The temperature decrease in the spinal cord is more than doubled when the surface temperature decreases from 20 to 0°C. At a cooling temperature of 20°C, $\Delta T_{sp} = 2.72$°C, while a 0°C cooling temperature results in a spinal cord temperature difference of 6.23°C. The 10°C pad surface temperature leads to $\Delta T_{sp} = 4.36$°C. Although all the three temperatures meet the design requirements ($\Delta T_{sp} \geq 2$°C), it may be more beneficial to use one of the two higher cooling temperatures. Using a cooling temperature of 0°C may lead to patient discomfort and possible freezing damage to the skin.

The blood perfusion rate in the spinal cord under normal conditions is 0.0083 s^{-1}, equivalent to 50 ml/min/100 g tissue. In this parametric study, the blood perfusion rate is either increased or decreased by 50%. The local blood perfusion as well as the metabolic heat generation act as a heat source during cooling. The results of this study demonstrate that decreasing the spinal blood perfusion rate by

Table 3 Parametric study results

Pad size		CSF velocity		Cooling temperature		Blood perfusion	
Width (mm)	ΔT_{sp} (°C)	u_{csf} (m/s)	ΔT_{sp} (°C)	T_{cool} (°C)	ΔT_{sp} (°C)	ω_{sp} (ml/100 g/min tissue)	ΔT_{sp} (°C)
350	2.72	**0.0764sin(2πt)**	**2.72**	**20**	**2.72**	75	2.24
300	2.72	0.0382sin(2πt)	2.91	10	4.36	**50**	**2.72**
200	2.72	0.0191sin(2πt)	3.05	0	6.23	25	3.41
100	**2.72**	–	–	–	–	–	–
50	2.58	–	–	–	–	–	–

Baseline model is highlighted by boldface

50% helps lower the spinal cord temperature from 34.17 to 33.48°C after 30 min of cooling, while increasing it hinders spinal cord cooling (34.66 vs. 34.17°C). Therefore, ischemia, often associated with secondary neuro-injury following traumatic spinal cord injury, will respond positively to the cooling protocol.

3 Discussion

Previous theoretical analyses and animal experiments have shown a decrease in blood perfusion in the spinal cord during both systemic and localized cooling, which helps increase the cooling penetration and assist in lowering the tissue temperatures [3, 4, 9, 41, 55]. We simulated only when the blood perfusion rate is compromised after ischemic injury, and our theoretical study has demonstrated the profound effect of local ischemia in the spinal cord in facilitating cooling penetration in the spinal cord. It is still not conclusive whether ischemia always occurs after SCI, but several experimental observations have illustrated an overall decrease in the local blood perfusion rate following traumatic SCI [12, 20, 41, 45, 46, 52]. It is also possible that the local blood perfusion rate may be affected by the temperature decrease in the spinal cord during cooling [11, 19, 52]. However, experiments performed by Bricolo et al. show that localized cooling increases spinal cord blood flow [8]. Future experimental studies are needed to further quantify not only the local temperature-dependent blood perfusion rate, but also the coupled relationship between blood flow and metabolism after injury.

Although the presented model can be considered the first step to developing a non-invasive cooling protocol to treat traumatic SCI, the developed model has some limitations. The version of FEMLAB® used in this study only utilizes tetrahedral elements for 3D meshing. Using hexahedral elements are popular in 3D finite element analyses because they may improve the accuracy of the model by increasing the number of nodes per element. However, hexahedral elements are usually used in solid mechanics analysis because these elements react more precisely to real-world loads and provide more accurate results in stress–strain analyses, especially for thin structures [10]. For 3D numerical heat transfer analyses, tetrahedral elements are preferred because they allow for unstructured and adaptive meshing schemes to discretize the domain completely and exactly, especially when analysis involves large Peclet numbers [22, 36].

We use the Pennes bioheat transfer equation to model the thermal effect of the local blood perfusion rate; therefore, the developed model inherits all the limitations associated with the Pennes continuum model. The modeled spinal cavity has a uniform cross-sectional area, which results in a constant CSF velocity in the axial direction. In reality, the fluid velocity decreases while it descends toward the spinal cavity due to an increase in the cross-sectional area [44]. Owing to the difficulty in modeling the detailed and irregular geometry using the FEM software, the geometrical representation of the actual structures is simplified to satisfy the overall heat transfer resistance by each tissue structure. For example, the peripheral spinal cord nerves have been neglected in this study. The spinal cord is connected to 33 pairs of nerves, and their addition would create a more complicated model to exceed our computational capacity. Also, there is no distinction between white and gray matter. The spinal cord has been simplified and modeled as a homogenous solid material. A more anatomically correct model would illustrate that the spinal cord is composed of an H-shaped gray matter surrounded by white matter. Such a representation could change the spinal cord temperature profiles since the blood perfusion rate and metabolic heat generation of the grey matter is approximately four times that of white matter [11, 49]. All the limitations associated with a simplification of the geometry can be addressed with improved software capability and computational memory capacity in the future. Developing a more detailed theoretical model provides the opportunity to more accurately describe temperature variations occurring at the injury site and the surrounding environment, which may be more beneficial to clinicians when implementing the cooling procedures. In addition to limitations due to the model geometry, there are

also limitations associated with the prescribed boundary conditions. In this model, the bottom surface of the torso is a constant temperature ($T = 37°C$), and an adiabatic boundary condition is prescribed on the top surface. Their effects on the temperature distribution during cooling can be examined if the torso model is incorporated with other parts of the body. However, as shown in a previous study by our group [49], it is unlikely that the effect will be significant since heat transfer is dominated in the lateral rather than the axial direction.

Intracranial pressure changes affect CSF motion in the spinal cavity. In this study, we are interested in how the fluid oscillations affect the heat transfer during cooling, even though there is a zero net flow rate. Fluids that undergo periodic oscillations have different flow and heat transfer characteristics than fluids with a steady flow have. The heat transfer rate is affected by changes in the boundary layer thickness, fluid mixing, and a lowered thermal resistance [16, 23]. Several previous studies in engineering design applications have concluded that the presence of an oscillating flow can enhance heat transfer by 15–40% and increase the effective thermal conductivity by 10–60% [16, 21, 30, 31, 53, 56]. It has been suggested that this enhancement is mainly due to the fact that oscillations promote fluid mixing and create vortices around the cylinder because the laminar-turbulent transition may be a major mechanism that enhances heat transfer in zero-mean oscillating flow [28, 31]. In convective heat transfer, the existence of an oscillatory layer of fluid is equivalent to an enhancement in heat transfer through convection. A majority of those previous studies seem to contradict our observation, where cooling penetration increases more with smaller oscillation intensities. We believe this may be partially due to a competing mechanism which involves the introduction of warm spinal fluid at 37°C from the sacral sac of the spinal cavity during the oscillation. The increasing amount of warm CSF entering the system counteracts the cooling effect, and may overpower the cooling enhancement due to fluid convection [23, 28]. Therefore, we believe it is reasonable to observe a decreased cooling penetration in the spinal cord when the oscillatory intensity is increased due to the large amount of warm CSF being introduced to the system.

4 Conclusion

The Pennes bioheat equation and FEM have been used to demonstrate that placing a cooling pad along the back of the torso is a feasible hypothermia treatment for secondary neuro-injuries associated with traumatic SCI. Theoretical analysis has shown that a simple cooling pad at 20°C can significantly decrease the temperatures of both the CSF and the spinal cord by more than 2.7°C within 30 min. Temperature reductions in the spinal cord are sensitive to the spinal cord blood perfusion rate, the cooling temperature, and the presence of oscillating CSF flow.

Acknowledgments This research was supported in part by the State of Maryland TEDCO fund, the LSAMP Bridge to the Doctorate Program, an NIGMS Initiative for Minority Student Development Grant (R25-GM55036), and Procter and Gamble. This research was performed by Katisha D. Smith in partial fulfillment of the requirements for the Ph.D. degree from the University of Maryland, Baltimore County.

References

1. Acosta-Rua G (1970) Treatment of traumatic paraplegic patients by localized cooling of the spinal cord. J Iowa Med Soc 60:326–328
2. Albin M, White R, Locke G (1965) Treatment of spinal cord trauma by selective hypothermic perfusion. Surg Forum 16:423–424
3. Albin M, White R, Yashon D et al (1968) Functional and electrophysiologic limitations of delayed spinal cord cooling after impact injury. Surg Forum 19:423–424
4. Albin M, White R, Acosta-Rua G et al (1968) Study of functional recovery produced by delayed localized cooling after spinal cord injury in primates. J Neurosurg 28:113–120
5. Balédent O, Henry–Feugeas M, Idy-Peretti I (2001) Cerebrospinal fluid dynamics and relation with blood flow: a magnetic resonance study with semiautomated cerebrospinal fluid segmentation. Invest Radiol 36:368–377
6. Battin M, Penrice J, Gunn T et al (2003) Treatment of term infants with head cooling and mild systemic hypothermia (35.0°C and 34.5°C) after perinatal asphyxia. Pediatrics 111:244–251
7. Black P, Van Devanter S, Cohn L (1976) Current research review: effects of hypothermia on systemic and organ system metabolism and function. J Surg Res 20:49–63
8. Bricolo A, Ore G, Da Pian R et al (1976) Local cooling in spinal cord injury. Surg Neurol 6:101–106
9. Casas C, Herrera L, Prusmack C et al (2005) Effects of epidural hypothermic saline infusion on locomotor outcome and tissue preservation after moderate thoracic spinal cord contusion in rats. J Neurosurg-Spine 2:308–318
10. Chandrupatla T, Belegundu A (2002) Introduction to finite elements in engineering. Prentice-Hall, Upper Saddle River
11. Diao C, Zhu L, Wang H (2003) Cooling and rewarming for brain ischemia or injury: Theoretical analysis. Ann Biomed Eng 31:346–353
12. Dimar J, Shields C, Zhang Y et al (2000) The role of directly applied hypothermia in spinal cord injury. Spine 25:2294–2302
13. Feinburg D, Mark A (1987) Human brain motion and cerebrospinal fluid circulation demonstrated with MR velocity imaging. Radiology 163:793–799
14. Goetz T, Romero-Sierra C, Ethier R et al (1988) Modeling of therapeutic dialysis of cerebrospinal fluid by epidural cooling in spinal cord injuries. J Neurotraum 5:139–150
15. Gray H (2001) Gray's anatomy: a facsimile. TAJ Books, London
16. Gül H (2007) Heat transfer in oscillating circular pipes. Exp Heat Transf 20:73–84
17. Hansebout R, Kuchner E, Romero-Sierra C (1975) Effects of local hypothermia and of steroids upon recovery from experimental spinal cord compression injury. Surg Neurol 4:531–536

18. Hansebout R, Tanner A, Romero-Sierra C (1984) Current status of spinal cord cooling in the treatment of acute spinal cord injury. Spine 9:508–511
19. Hansebout R, Lamont R, Kamath M (1985) The effects of local cooling on canine spinal cord blood flow. Can J Neurol Sci 12:83–87
20. Hausmann O (2003) Post-traumatic inflammation following spinal cord injury. Spinal Cord 41:369–378
21. Hemida H, Sabry M, Abdel-Rahim A et al (2002) Theoretical analysis of heat transfer in laminar pulsating flow. Int J Heat Mass Transf 45:1767–1780
22. Hirsch C (1988) Numerical computation of internal and external flows. John Wiley & Sons, New York
23. Huang P, Nian S, Yang C (2005) Enhanced heat-source cooling by flow pulsation and porous block. J Thermophys Heat Transf 19:460–470
24. Hulsebosch C (2002) Recent advances in pathophysiology and treatment of spinal cord injury. Adv Physiol Educ 26:238–255
25. Inamasu J, Nakamura Y, Ichikizaki K (2003) Induced hypothermia in experimental traumatic spinal cord injury: an update. J Neurol Sci 209:55–60
26. Incropera F, DeWitt D (1996) Fundamentals of heat and mass transfer, 4th edn. John Wiley and Sons, New York
27. Isaka M, Kumagai H, Sugawara Y et al (2006) Cold spinoplegia and transvertebral cooling pad reduce spinal cord injury during thoracoabdominal aortic surgery. J Vasc Surg 43:1257–1262
28. Iwai H, Mambo T, Yamamoto N et al (2004) Laminar convective heat transfer from a circular cylinder exposed to a low frequency zero-mean velocity oscillating flow. Int J Heat Mass Transf 47:4659–4672
29. Kwun B, Vacanti F (1995) Mild hypothermia protects against irreversible damage during prolonged spinal cord ischemia. J Surg Res 59:780–782
30. Leong K, Jin L (2005) An experimental study of heat transfer in oscillating flow through a channel filled with aluminum foam. Int J Heat Mass Transf 48:243–253
31. Li P, Yang K (2000) Mechanisms for the heat transfer enhancement in zero-mean oscillatory flows in short channels. Int J Heat Mass Transf 43:3551–3566
32. Loth F, Yardimci M, Alperin N (2001) Hydrodynamic modeling of cerebrospinal fluid motion within the spinal cavity. J Biomech Eng 123:71–79
33. Maganæs B (1989) Clinical studies of cranial and spinal compliance and the craniospinal flow of cerebrospinal fluid. Br J Neurosurg 3:659–668
34. Marsala M, Galik J, Ishikawa T et al (1997) Technique of selective spinal cord cooling in rat: methodology and application. J Neurosci Methods 74:97–106
35. Martinez-Arizala A, Green B (1992) Hypothermia in spinal cord injury. J Neurotram 9:S497–S505
36. Minkowycz W, Sparrow E (1997) Advances in numerical heat transfer. Taylor & Francis, Washington DC
37. Mori A, Ueda T, Hachiya T et al (2005) An epidural cooling catheter protects the spinal cord against ischemia injury in pigs. Ann Thorac Surg 80:1829–1834
38. O'Connell J (1943) Vascular factor in intracranial pressure and maintenance of cerebro-spinal fluid circulation. Brain 66: 204–228
39. Polderman K (2004) Application of therapeutic hypothermia in the ICU: opportunities and pitfalls of a promising treatment modality. Part 1: indications and evidence. Intensive Care Med 30:556–575
40. Prytherch D, Smith M, Williams B (1979) The measurement of cerebrospinal fluid flow. Phys Med Biol 24:1196–1208
41. Reyes O, Sosa I, Kuffler D (2003) Neuroprotection of spinal neurons against blunt trauma and ischemia. Puerto Rico Health Sci J 22:277–286
42. Rubini L, Colombo F (1981) Modified technique for local cooling in spinal cord injuries. Spine 6:417–419
43. Saunders N, Habgood M, Dziegielewska K (1999) Barrier mechanisms in the brain. Clin Exp Pharmacol Physiol 26:11–19
44. Schellinger D, LeBihan D, Rajan S et al (1992) MR of slow CSF flow in the spine. Am J Neuroradiol 13:1393–1403
45. Taoka Y, Okajima K (1998) Spinal cord injury in the rat. Prog Neurobiol 56:341–358
46. Tator C (1972) Acute spinal cord injury: a review of recent studies of treatment and pathophysiology. Can Med Assoc J 107:143–150
47. Thienprasit P, Bantli H, Bloedel J et al (1975) Effect of delayed local cooling on experimental spinal cord injury. J Neurosurg 42:150–154
48. Tsutsumi K, Ueda T, Shimizu H et al (2004) Effect of delayed induction of postischemic hypothermia on spinal cord damage induced by transient ischemic insult in rabbits. Jpn J Thorac Cardiovasc Surg 52:411–418
49. Wang Y, Zhu L (2007) Targeted brain hypothermia induced by an interstitial cooling device in human neck: theoretical analyses. Eur J Appl Physiol 101:31–40
50. Wang L, Yan Y, Zou L et al (2005) Moderate hypothermia prevents neural cell apoptosis following spinal cord ischemia in rabbits. Cell Res 15:387–393
51. Wells J, Hansebout R (1978) Local hypothermia in experimental spinal cord trauma. Surg Neurol 10:200–204
52. Westergren H, Farooque M, Olsson Y et al (2001) Spinal cord blood flow changes following systemic hypothermia and spinal cord compression injury: an experimental study in the rat using Laser-Doppler flowmetry. Spinal Cord 39:74–84
53. Xian H, Liu D, Shang F et al (2007) Study on heat transfer enhancement of oscillating-flow heat pipe for drying. Dry Technol 25:723–729
54. Xu X, Tikuisis P, Giesbrecht G (1999) A mathematical model for human brain cooling during cold-water near-drowning. J Appl Physiol 86:265–272
55. Yashon D, Vise W, Dewey R et al (1973) Temperature of the spinal cord during local hypothermia in dogs. J Neurosurg 39:742–745
56. Zhang X, Maruyama S, Sakai S (2004) Numerical investigation of laminar natural convection on a heated vertical plate subjected to a periodic oscillation. Int J Heat Mass Transf 47:4439–4448
57. Zhu L (2002) Chapter 2: bioheat transfer. In: Standard handbook of biomedical engineering and design. McGraw-Hill, New York
58. Zhu L, Diao C (2001) Theoretical simulation of temperature distribution in the brain during mild hypothermia treatment for brain injury. Med Biol Eng Comput 39:681–687